Available online at www.sciencedirect.com
ScienceDirect
International Journal of Fatigue xxx (2007) xxx–xxx
International Journal of Fatigue
www.elsevier.com/locate/ijfatigue

Course of SN-curves especially in the high-cycle fatigue regime with regard to component design and safety

C.M. Sonsino *

Fraunhofer-Institute for Structural Durability and System Reliability, LBF, Bartningstrasse 47, 64289 Darmstadt, Germany

Received 22 May 2006; received in revised form 30 October 2006; accepted 23 November 2006

Abstract

Conventional design codes base their recommendations still on the common prejudice that an ''endurance limit'' exists. However, several investigations prove clearly that in the high-cycle regime a decrease of fatigue strength with increased number of cycles still occurs, even if corrosion or temperature effects are excluded. Therefore, the fatigue design of components submitted to loadings below the knee point of the SN-curve must consider this fact in order to avoid failures. With regard to the course of the SN-curve in the very high-cycle area, material and manufacturing dependent recommendations are given.

Keywords: SN-curve; High-cycle fatigue; Giga-cycle fatigue; Steel; Aluminium; Magnesium; Welded joints; Safety

1. Introduction

Fatigue strength is subdivided in different regions, Fig. 1, while especially the high-cycle behaviour of materials and components is still discussed very controversially with regard to the course of the SN-curve in this regime. Especially, the expression ''endurance limit'' or ''fatigue limit'', in German ''Dauerfestigkeit'', in French ''limite d'endurance'', etc., still misleads many design engineers into assuming that a structural element will not fail as long as the so-called fatigue limit is not exceeded, Fig. 2. This assumption is semantically implied by the English term ''limit'' as well as by the German term ''Dauer'' (duration) and is a part of several design regulations [1–5] and more.

The existence of a steadily decreasing fatigue strength beyond the knee point of the SN-curve in the range of high cycles observed for materials like aluminium or austenitic steels with face centred cubic structures has always been the state-of-the-art, but for materials with body centred cubic structures such as ferritic steels the existence of a ''fatigue limit'' has always been claimed. Various design regulations and standards point out [2–6] that a ''fatigue limit'' does not exist in the case of

- jointed components, such as press-fits of railway-wheelsets [7] or bolted joints because of fretting corrosion, Fig. 3,
- high temperatures, and/or
- corrosive environments [8] if a passivation of the surface does not occur, Fig. 4.

It is also common knowledge that welded joints under axial loading or bending, due to residual tensile stresses, and under torsion exhibit decreasing fatigue strength at load levels leading to more than 10^7 load cycles. Some regulations [4,5] take this into account up to 5×10^6 cycles but show constant fatigue strength at larger number of cycles, thus allowing the use of a non-existent fatigue limit.

For structural and heat treatable steels with ferritic, bainitic or martensitic microstructure, a ''fatigue limit'' is

* Tel.: +49 61 51/7 052 44; fax: +49 61 51/7 052 14.
E-mail address: c.m.sonsino@lbf.fraunhofer.de

0142-1123/$ - see front matter © 2006 Elsevier Ltd. All rights reserved.
doi:10.1016/j.ijfatigue.2006.11.015

Nomenclature

D	damage sum	T	scatter
N	cycle		
f	frequency	*Indexes*	
P	probability	a	amplitude
j	safety factor	n	nominal
ς	density	cr	crack
k, k^*, k'	slopes of the SN-curve	o	occurrence
R	load or stress ratio	E	endurance
L_s	sequence length	r	rupture
R_z	roughness	f	failure
K_t	stress concentration factor	s	survival
σ	stress	k	knee
K_{th}	threshold stress intensity	S	service
s	thickness		

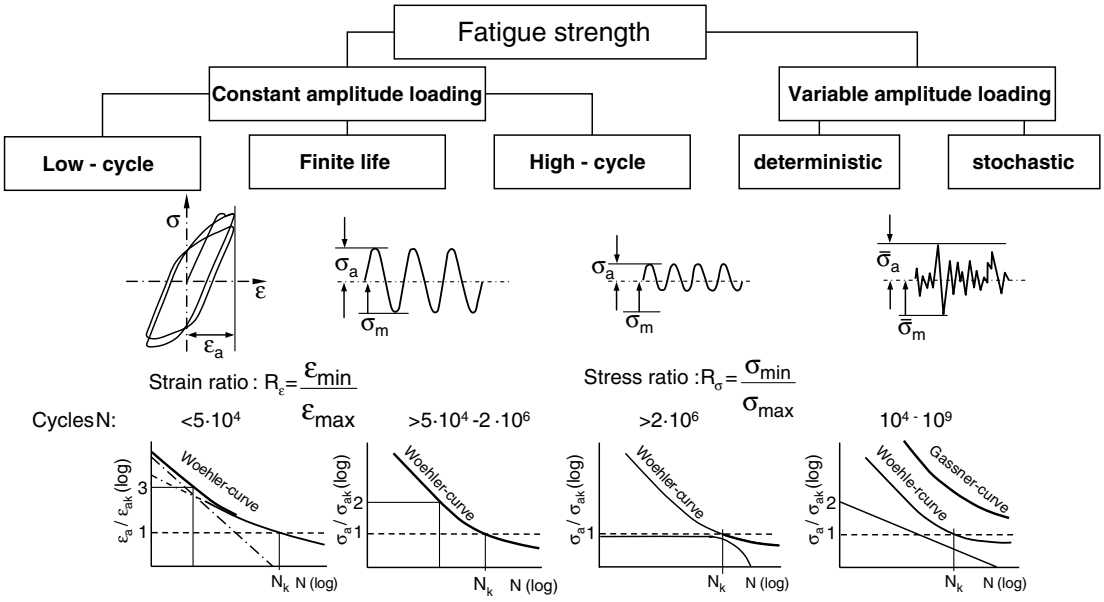

Fig. 1. Partition of fatigue strength.

still believed to be exhibited except when environmental effects exist. Thus, for structural parts like connecting rods, crankshafts, and helical springs being subjected to far more than 10^6 service peak load cycles, experiencing during their total service life up to 10^{10} cycles and designed such that corresponding maximum peak stresses stay below the so-called "endurance limit", only the application of suitable safety factors prevents fracture, Fig. 2. Structural durability designing to withstand variable amplitude loadings also allows loading in the range of finite life fatigue strength, i.e. exceeding of the so-called "endurance limit", to obtain a lightweight structure, Fig. 5. In this case, the drop of fatigue strength in the high-cycle range is considered using Woehler-curves for the damage calculation with fictitious slopes beyond the knee point[1] of $k' = 2k - 1$ or $2k - 2$ (according to Haibach [9]) depending on material condition (wrought, cast or welded). Therefore, here it is not necessary to know the real shape of the Woehler curve in the high-cycle regime.

In this context, it should be mentioned that about 65 years ago for constant amplitude design the use of the fatigue strength amplitude to be determined at $N = 10^8$ cycles was recommended already for different steels and aluminium alloys of that time [10]. Obviously, the inten-

[1] Physically a knee point does not exist, as the Woehler-curves change their slope fluently in the transition range (from finite to high-cycle fatigue strength). The knee point is solely a parameter for strength estimations.

Please cite this article in press as: Sonsino CM, Course of SN-curves especially in the high-cycle fatigue regime ..., Int J Fatigue (2007), doi:10.1016/j.ijfatigue.2006.11.015

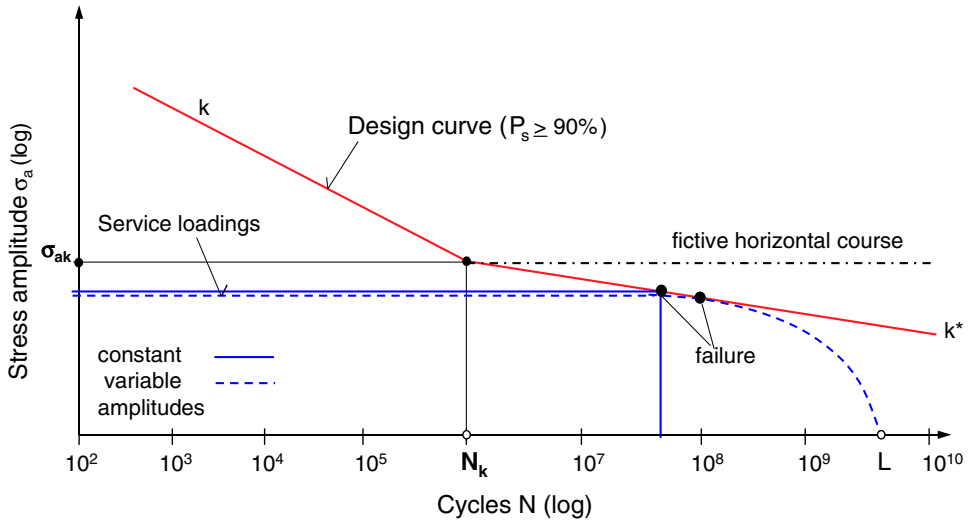

Fig. 2. Design against the so-called "endurance limit".

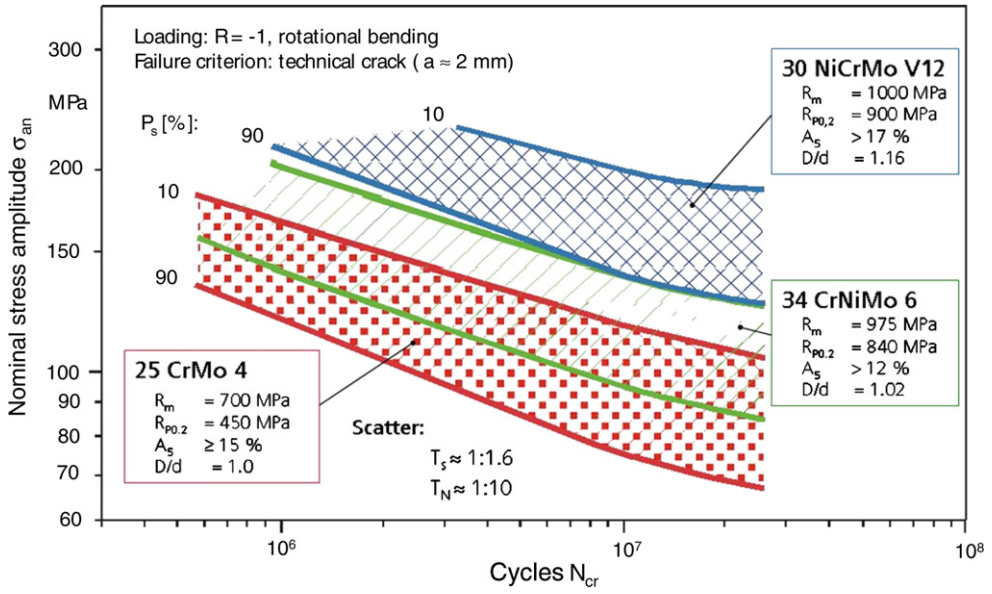

Fig. 3. Fatigue strength of the railway-wheelsets at press-fits (constant amplitude loading).

tion was to consider by this the decrease of fatigue strength at least up to 10^8 cycles with the testing possibilities of that time.

In the following, an exemplary presentation of selected, not commonly known results up to $N = 10^{11}$ cycles will be made, disproving the existence of a fatigue limit, and suggestions will be made to consider fatigue behaviour under real or idealized constant amplitude loading in the range of large number of cycles if an experimental proof is not feasible. The decrease of fatigue strength in this range is caused by failure mechanisms related to microstructural phenomena occurring more or less at macroscopic elastic deformations [11,14,17,21–23].

Consequently, a "fatigue limit" is realistic only if no damage-causing microstructural defects and no aggressive surface conditions exist.

2. Examples of decreasing fatigue strength in the range of high cycles

Whereas conventional servo-hydraulic fatigue testing machines, resonant actuators and shakers run at maximum frequencies up to 400 Hz, ultrasonic test machines allow frequencies to be larger by a factor of 100, i.e. up to 40 kHz; thereby it is feasible to conduct tests in the range of giga cycles (10^9) up to 10^{12} within a suitable testing time [11–20] and others. However, this principle of testing has some restrictions, as for example:

- Testing is only feasible with small specimens ($d <$ 10 mm).
- Despite cooling, self-heating in the specimen core must be considered.

Please cite this article in press as: Sonsino CM, Course of SN-curves especially in the high-cycle fatigue regime ..., Int J Fatigue (2007), doi:10.1016/j.ijfatigue.2006.11.015

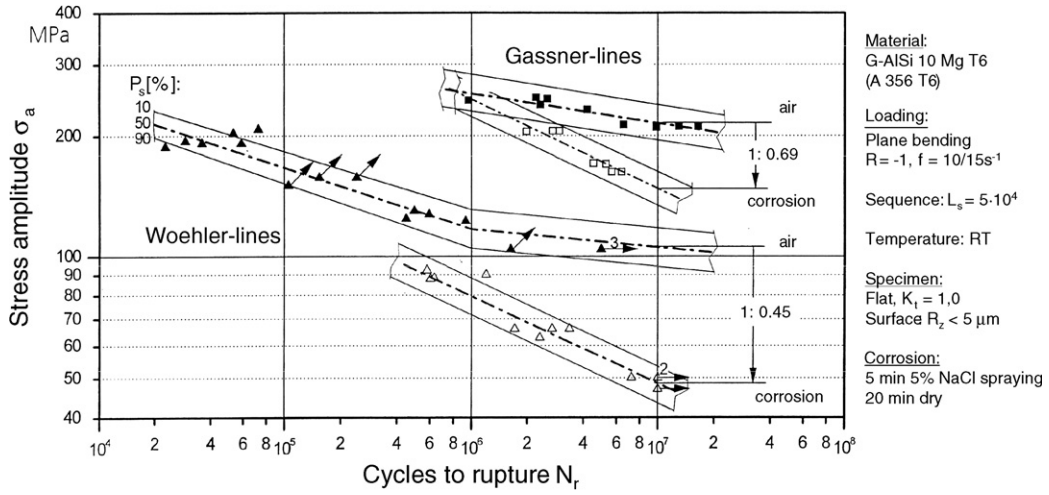

Fig. 4. Influence of the salt-spray corrosion on the fatigue strength of cast aluminium under constant and variable amplitude loading.

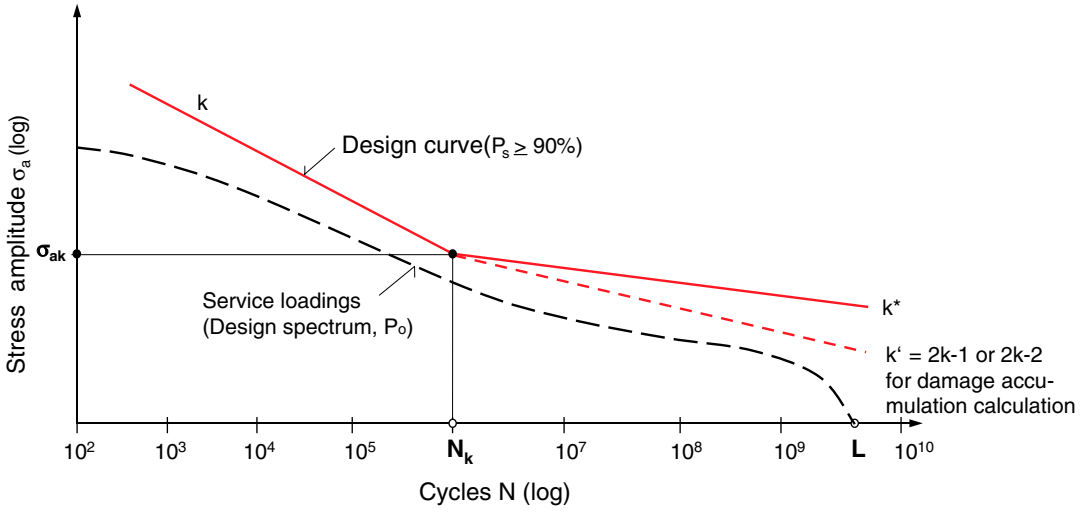

Fig. 5. Design against variable amplitudes (spectrum loading).

- Load monitoring is inaccurate at $N < 10^6$ because of the very short control time.
- A fluent transition of results from low frequency testing with those from ultrasonic frequency testing is not always possible [16,17].

Despite these difficulties the application of this technique indicates and evaluates correct tendencies regarding the decrease of fatigue strength and the apparent failure mechanisms [14,21]. Furthermore, results more recently derived from 400 and 20 Hz testing in the high-cycle regime will be considered. However, only the outcomes of the 400 Hz tests resulting in lives $N > 10^6$ should be evaluated because of the difficulties of correct load adjustment below 10^6 cycles.

In the following, this paper shows Woehler-curves from 10 materials, Tables 1 and 2, often applied by the automotive and aircraft industry. The materials are as follows the following:

- the precipitation hardening steel 38MnVS6 BY for the fabrication of connecting rods and crankshafts,
- cast nodular iron GGG 50 for the fabrication of hubs and steering parts,
- steel 100Cr6 for ball bearings,
- cast aluminium alloy G-AlSi5Cu3Mg0.4 T5 for crankshaft housings and motor bearings,
- sintered steel Fe–4.0Ni–1.5Cu–0.5Mo + 0.5C for gear parts such as synchronizing hubs and levers,
- wrought aluminium alloys AlCuMg2 T351 and AlZnMgCu1.5 T66 of aircraft structures,
- wrought aluminium alloy AlMgSi1 T6 for load carrying car components,
- cast magnesium alloy MgAl9Zn1 for housings, and
- the shot-peened high-strength spring steel SiCr for helical springs.

Compared to their presentation in the primary literature [12–23], here the important design characteristics slope of

Table 1
Materials and chemical composition

Materials	DIN Code	C	Si	Mn	P	S	Mo	Cr	Ni	Cu	G	Ai	V	Mg	Fe	Zn	Ti	Pb	Sn
1	38 MnVS6 BY	0.38	0.567	1.23	0.012	0.064	0.018	–	0.063	0.063	0.183	0.025	0.089	–	Rest	–	–	–	–
2	GGG50	3.65	2.49	0.50	–	–	–	–	–	0.70	–	–	–	0.04	Rest	–	–	–	–
3	100Cr6	1.03	0.24	0.34	–	0.008	0.03	1.46	0.15	–	–	–	–	–	Rest	–	–	–	–
4	G-AlSi5Cu3Mg0.4 T5	–	5.30	0.32	–	–	–	–	0.03	3.15	–	Rest	–	0.36	0.55	0.17	0.11	0.02	115 ppm
5	Fe-4.ONi-1.5Cu.0.5Mo+0.5C	0.5	–	–	–	–	0.50	–	4.00	1.50	–	–	–	–	Rest	–	–	–	–
6	AlCuMg2 T351	–	1.00	0.70	–	–	–	<0.05	–	4.50	–	–	–	1.50	0.20	<0.05	<0.03	–	–
7	AlZnMgCu1.5 T66	–	0.14	0.07	–	–	–	0.02	–	1.73	–	–	–	2.72	0.27	7.26	0.06	–	–
8	AlMgSi T6	–	1.00	0.70	–	–	–	<0.25	–	<0.10	–	–	–	0.90	<0.50	<0.20	<0.10	–	–
9	MgAl9Zn1	–	0.002	0.114	–	–	–	–	0.005	0.002	–	8.69	–	–	0.022	0.906	–	–	–
10	VDSiCr	0.55	1.40	0.70	<0.025	<0.02	–	0.65	–	<0.006	–	–	0.20	–	Rest	–	–	–	–

Table 2
Materials and mechanical data

Material	DIN Code	International standard	$R_{po.2}$ in MPa	R_m in MPa	A_5 in %	E in GPa	Hardness
1	38MnVS6	NF EN 10267	608	878	20	210	246 HV30
2	GGG50	NF EN 1563	460	795	9	170	265 HV30
3	100Cr6	AISI-SAE 52100 NF EN ISO 687-17	–	2300	–	210	780 HV30 63 HRc
4	G-AlSi5Cu3Mg0.4 T5	NF EN 1780-2	182	222	1	72	99 HV30
5	Fe–4.0Ni–1.5Cu–0.5Mo +0.5C (35 min/1120 °C) $\varsigma = 7.28$ g/cm^3	–	–	1005	–	155	336 HV30
6	AlCuMg2 T351	AA 2024	352	460	18	72	128 HV30
7	AlZnMgCu1.5 T66	AA 7075	606	641	4	71	185 HV30
8	AlMgSi1 T6	AA 6082 T6	240	340	9.0	70	–
9	MgAl9Zn1	Zn1 AZ 91	139	199	1.3	40	68 HV0.01
10	VDSiCr	–	–	2216	–	206	–

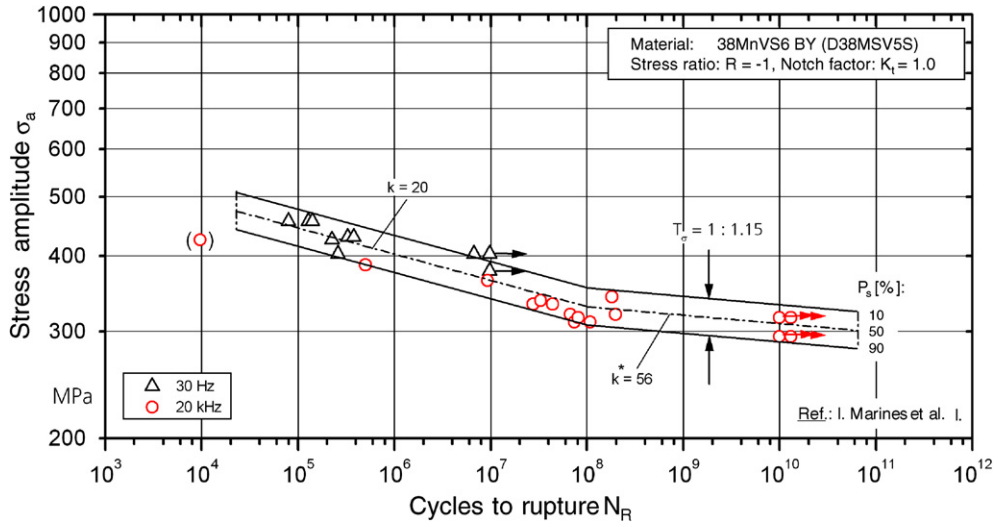

Fig. 6. SN-curve of a precipitation hardening steel up to the giga-cycle regime.

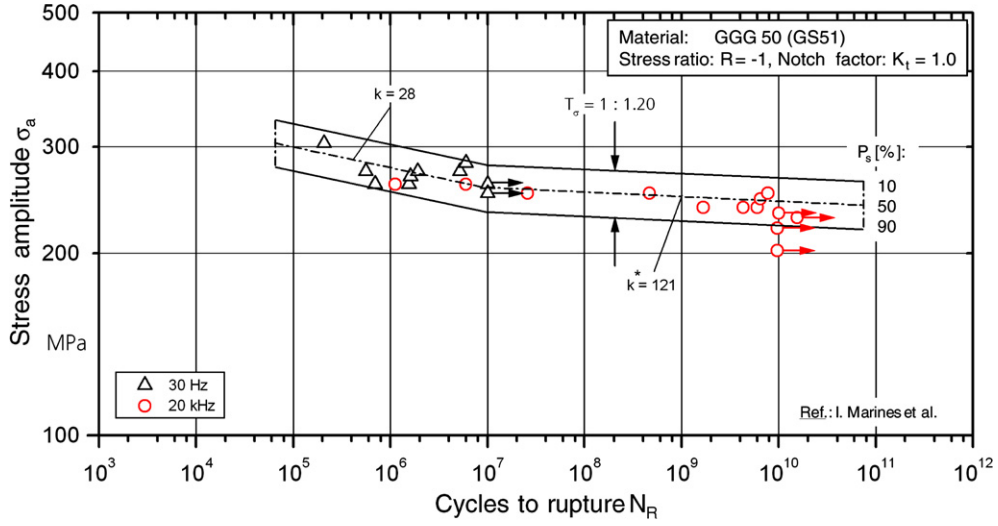

Fig. 7. SN-curve of a cast iron up to the giga-cycle regime.

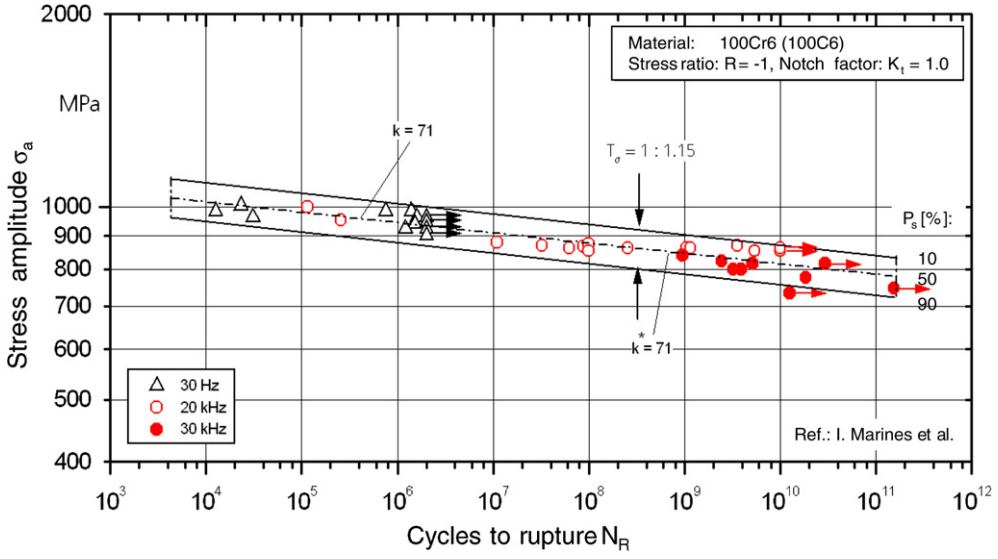

Fig. 8. SN-curve of a martensitic steel up to the giga-cycle regime.

Please cite this article in press as: Sonsino CM, Course of SN-curves especially in the high-cycle fatigue regime ..., Int J Fatigue (2007), doi:10.1016/j.ijfatigue.2006.11.015

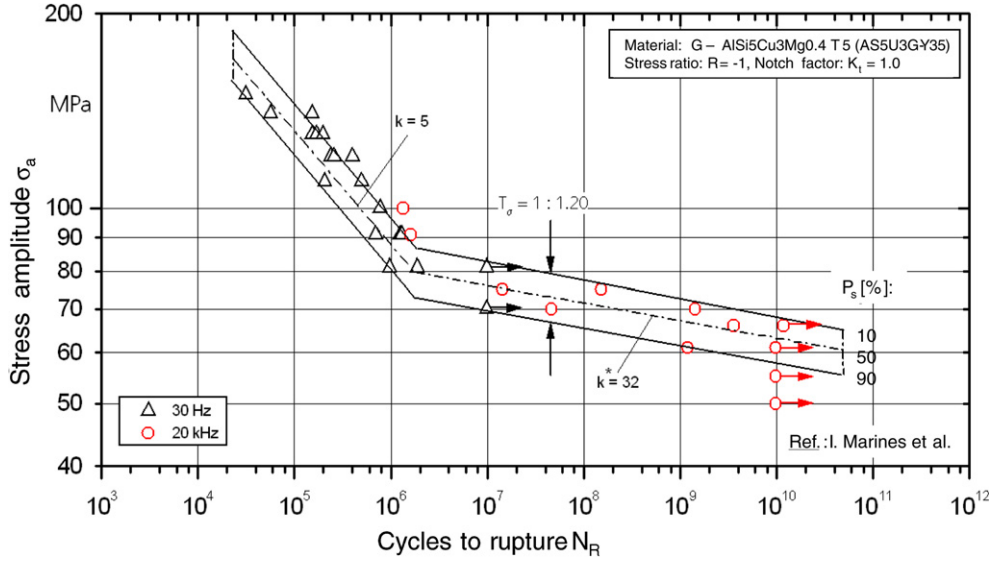

Fig. 9. SN-curve of a cast aluminium alloy up to the giga-cycle regime.

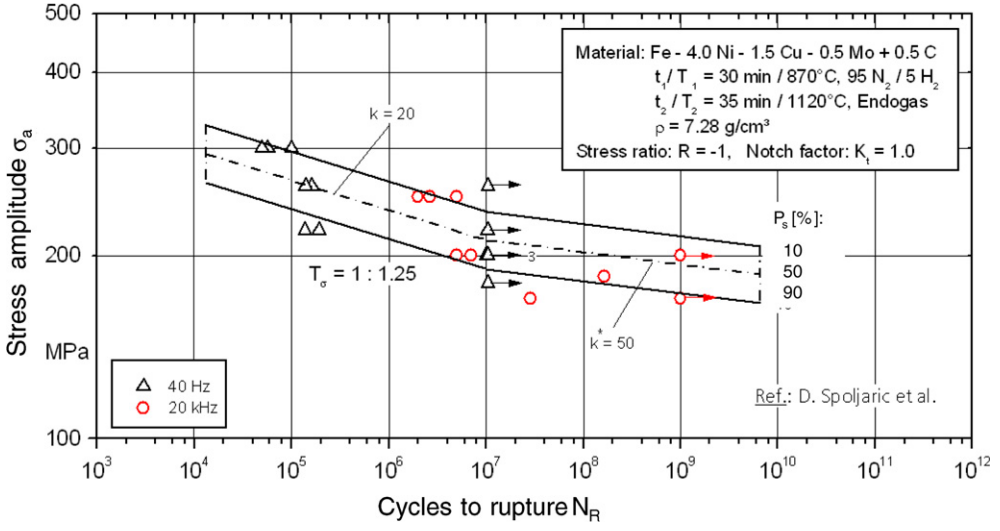

Fig. 10. SN-curve of a sintered steel up to the giga-cycle regime.

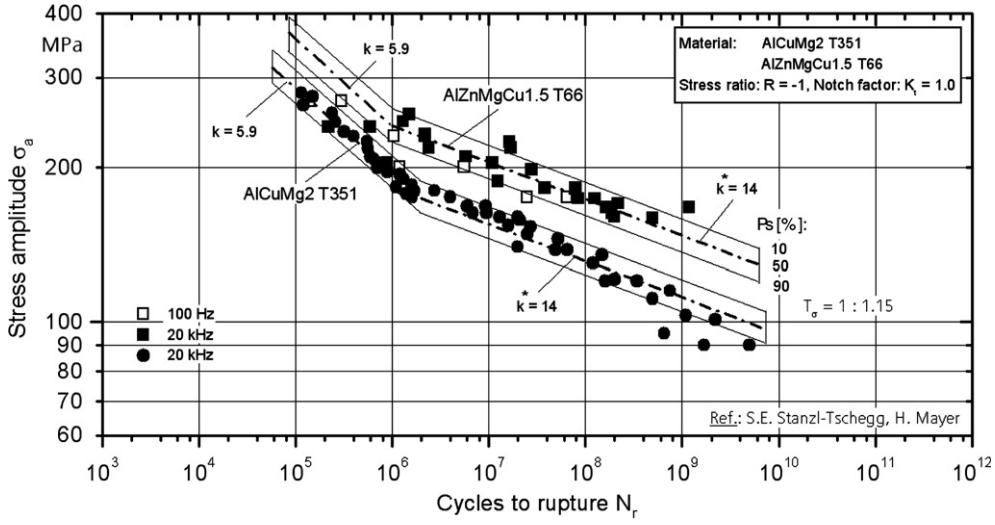

Fig. 11. SN-curve of two aluminium alloys up to the giga-cycle regime.

Please cite this article in press as: Sonsino CM, Course of SN-curves especially in the high-cycle fatigue regime ..., Int J Fatigue (2007), doi:10.1016/j.ijfatigue.2006.11.015

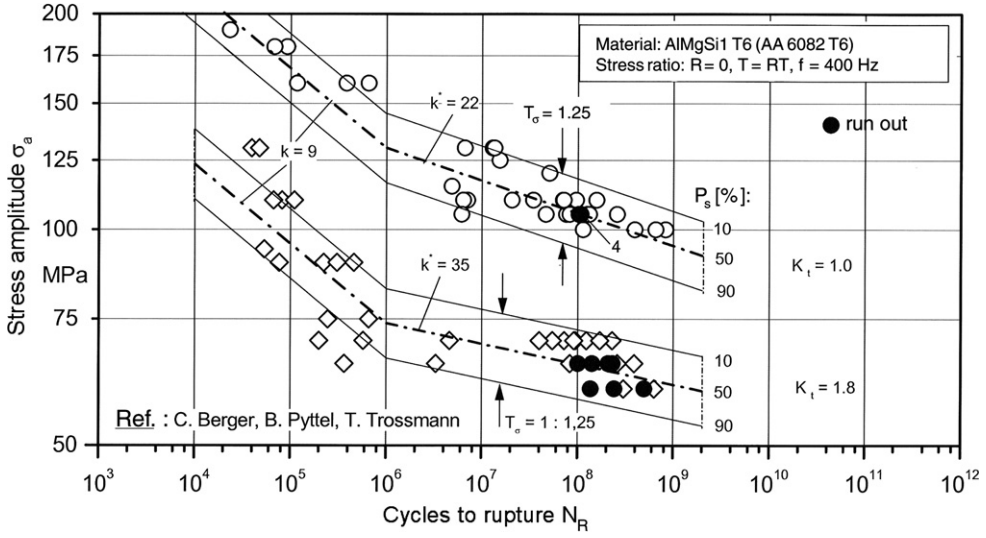

Fig. 12. SN-curves of a wrought aluminium alloy up to the giga-cycle regime.

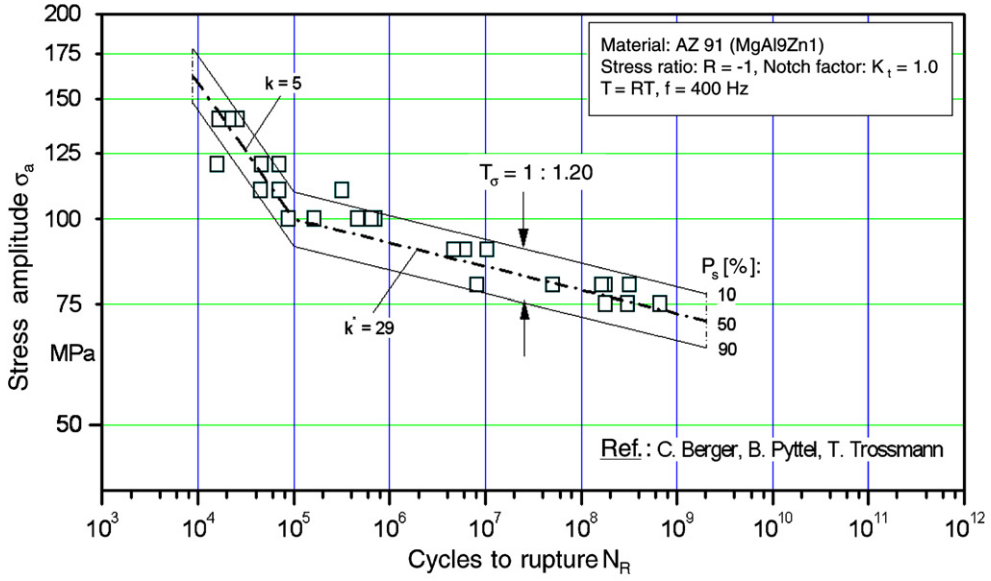

Fig. 13. SN-curve of cast magnesium alloy up to the giga-cycle regime.

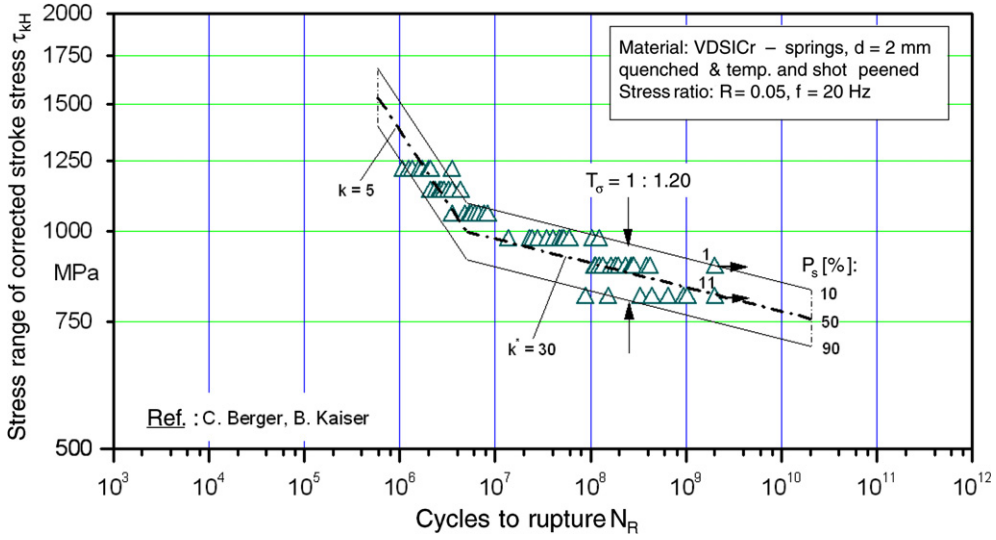

Fig. 14. Fatigue strength of shot-peened springs up to the giga-cycle regime.

Please cite this article in press as: Sonsino CM, Course of SN-curves especially in the high-cycle fatigue regime ..., Int J Fatigue (2007), doi:10.1016/j.ijfatigue.2006.11.015

the Woehler-curves, knee points, and scatters presented in a double logarithmic plot are now newly evaluated, Figs. 6–14.

The failure criterion of the illustrated test results is total specimen fracture. Crack propagation velocity as well as crack propagation life up to an initial crack size of $a = 0.5$ mm and beyond were generally not considered here. A corresponding differentiation of the total fatigue life regarding the evaluation of cracks in relation to complex conditions such as stress gradients and larger specimen size would have been advisable.

3. Evaluation of the examples

The slopes ahead and beyond the knee point, k and $k^* = \lg(N_2/N_1)/\lg(\sigma_{a1}/\sigma_{a2})$, respectively, result from linear regression analyses as well as curve fitting. Following the concept of normalized Woehler-curves [9], the test results were covered by scatter bands with uniform scatter bands $T_\sigma = 1{:}[\sigma_a(P_s = 10\%)/\sigma_a(P_s = 90\%)]$ based on experiences [24–30] and depending on the material. All Woehler-curves shown and the evaluation of the other results [27–29,31] reveal a continuous decrease of fatigue strength in the range of large cycle numbers. Many materials such as the martensitic steel 100Cr6, Fig. 8, exhibit no knee point at all. With the slope k^* the decrease of fatigue strength per decade is determined, Table 3.

Table 3
Decrease of fatigue strength per decade in the region of high cycles

Materials	DIN Code	k^*	Decrease of fatigue strength per decade in %
1	G-AlSi5Cu3Mg0.4 T5	32	7
2	GGG50	121	2
3	38 MnVS6 BY	56	4
4	100Cr6	71	3
5	Fe–4.ONi–1.5Cu.0.5Mo + 0.5C, $\varsigma = 7.28$ g/cm^3	50	~5
6	AlCuMg 2 T351	14	15
7	AlCuMg1.5 T66	14	15
8	AlMgSi T6	22	10
9	MgAl9Zn1	29	~8
10	VDSiCr	30	~8

The observed decrease per decade after the knee point or in the high-cycle range is below 5% for steels and below 10% for aluminium alloys. These results support practical experiences at hand [23,33]. However, the decrease per decade of fatigue strength for the aluminium alloy of about 15% is extraordinarily large compared to the investigations with the ordinary test machines (up to 10^7 cycles), which lead also to values below 10% [32].

4. Recommendations and final conclusions

Under the premise that no environmental or fretting corrosion is present and in the case that testing up to the range of giga cycles is not possible, a Woehler-curve representing results from tests with normal frequencies ($f <$ 50 Hz) in the finite life range may be extrapolated into the long life range beyond the knee point N_k with the following slope data:

- For steels, cast irons and magnesium alloys $k^* = 45$ corresponding to a decrease of 5% per decade if no large tensile residual stresses are present.
- For aluminium alloys welded magnesium alloys, and welded steels $k^* = 22$ corresponding to a decrease of 10% per decade.

The position of the knee point depends on the material (alloy), on its strength and also on the kind of loading

Table 4
Recommended knee points, slopes after the knee point and scatters

Material	N_k	k^*	Decrease per decade	$1{:}T_\sigma$
Steel, not welded	5×10^5, high strength 2×10^6, structural steels	45	5	1.20
Steel, welded	1×10^6, thermal stress relieved 1×10^7, high tensile residual stresses	45 22	5 10	1.50
Cast steel	5×10^5, high strength 2×10^6, medium strength	45	5	1.40
Sintered steel	5×10^5, high strength 2×10^6, medium strength	45	5	1.25
Cast nodular iron	5×10^5, high strength 2×10^6, medium strength	45	5	1.40
Wrought aluminium alloys,not welded	1×10^6–5×10^6	22	10	1.25
Wrought aluminium alloys, welded	1×10^6 thermal stress relieved 1×10^7, high tensile residual stresses	22	10	1.45
Cast aluminium	1×10^6–5×10^6	22	10	1.40
Sintered aluminium	1×10^6	22	10	1.25
Wrought magnesium alloys, not welded	5×10^4–1×10^5	45	5	1.20
Cast magnesium	1×10^5–5×10^5	45	5	1.30
Wrought magnesium alloys, welded	5×10^5, low tensile residual stresses 1×10^7, high tensile residual stresses	22	10	1.50

Please cite this article in press as: Sonsino CM, Course of SN-curves especially in the high-cycle fatigue regime ..., Int J Fatigue (2007), doi:10.1016/j.ijfatigue.2006.11.015

(axial, bending, torsion, stress ratio) [2,7,22,34–36] and, in the case of welded joints, additionally on the magnitude of the residual stresses [37,38]. The scatter T_σ fixed to a given mean value and required to derive safety factors and corresponding allowable strength data [9] depends decisively on material quality (pureness, population of defects); Table 4 presents some details.

Based on these findings and on the observed decrease of fatigue strength beyond 10^7 cycles reported in other investigations [39–43], the existing IIW – Recommendations for the structural durability designing of welded components [43] have already been revised [44], Figs. 15–17.

The data given in Fig. 15 were obtained with fillet welded longitudinal stiffeners, butt welded plates and girth welded tubes. They were tested under the stress ratios $R = -1$, 0 and >0. The testing frequency for the longitudinal stiffeners was $f = 125$ Hz, for the butt welds and tubes between 10 and 30 Hz.

For the sake of completeness, supplementary details to the Woehler-curve slope ahead the knee point are offered here also for components, because they contain notches leading to steeper slopes in the finite life range depending on material. Due to the more or less macroscopic elastic deformations, the slope is not significantly influenced in the long life range. By this aspect, slope data for the finite

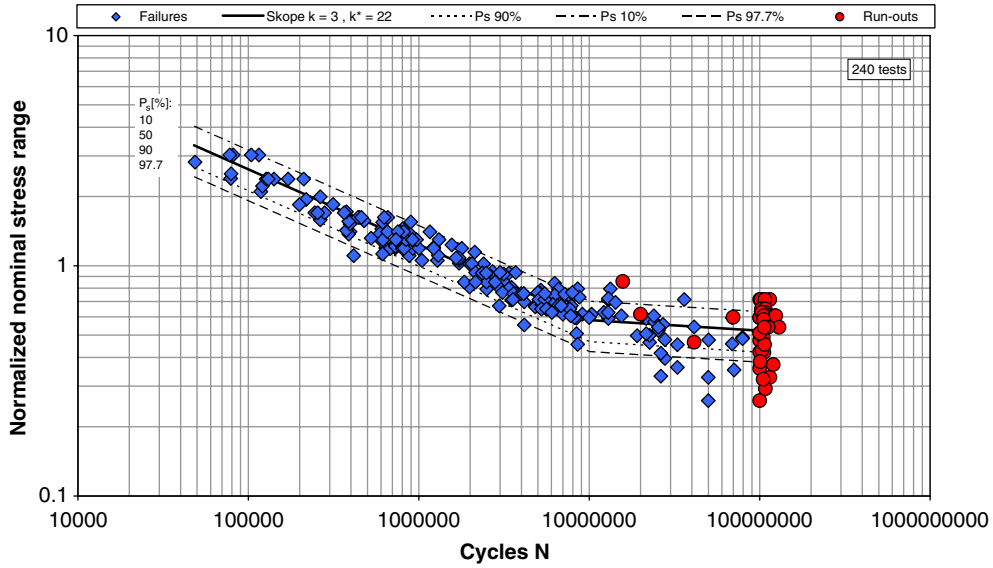

Fig. 15. Overall normalized evaluation and comparison with the proposed course of the SN-curve for welded steel joints.

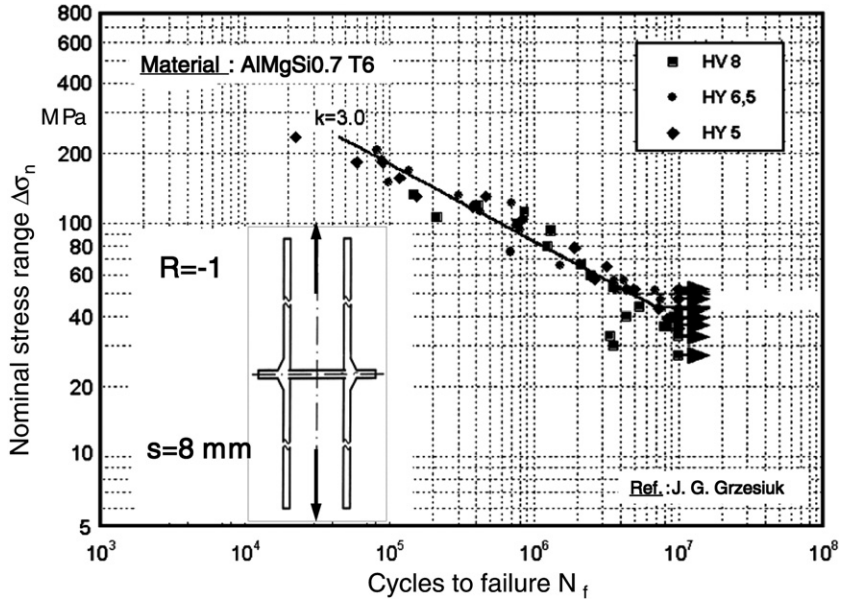

Fig. 16. Fatigue test results with H-type welded aluminium specimens.

Please cite this article in press as: Sonsino CM, Course of SN-curves especially in the high-cycle fatigue regime ..., Int J Fatigue (2007), doi:10.1016/j.ijfatigue.2006.11.015

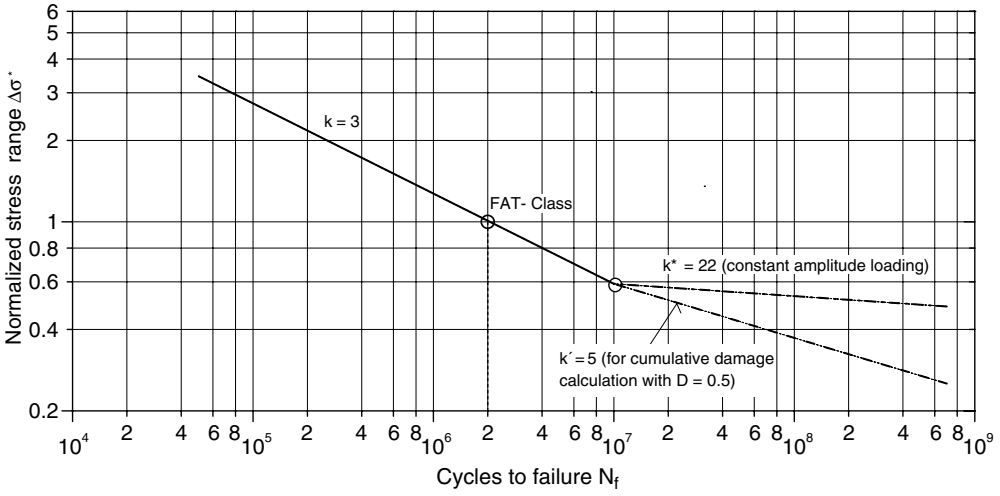

Fig. 17. SN-curve for welded joints according to IIW-Recommendations.

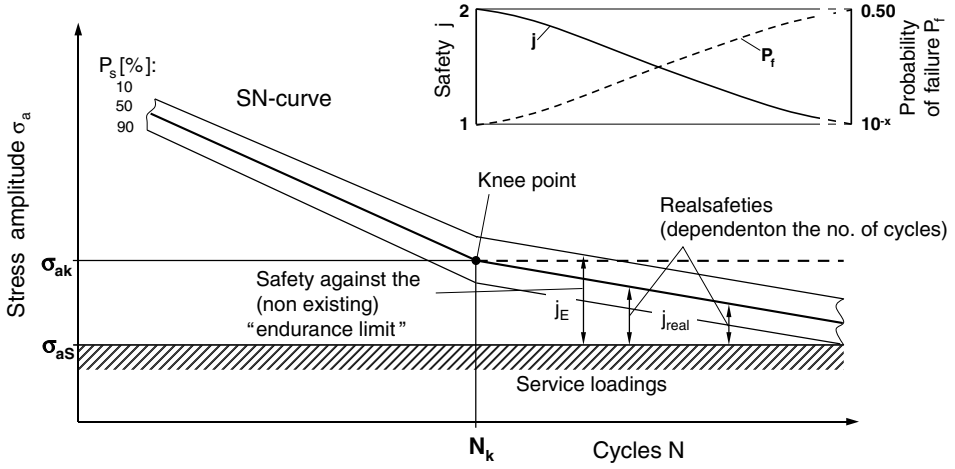

Fig. 18. Real and non-existent safeties at a design against the "endurance limit".

life range ($N < N_k$) of $k = 5$ up to 8 are proposed for non-welded components of steel, cast steel, cast nodular iron, sintered steel, aluminium, and magnesium alloys. For welded thin-walled components and structures made of steel as well as aluminium and magnesium alloys $k = 5$–8, and for welded thick-walled components and structures $k = 3$–5 may be applied.

As a consequence of the knowledge gained, one should be aware, when traditionally designing against a so-called "endurance limit", that the continuous decrease of fatigue strength diminishes the real safety[2] j_{real} (N) under service loading with increasing number of load cycles, Fig. 18, and thereby increases the failure probability P_f.

Many in-service failures of components like connecting rods, crankshafts, helical springs, shafts of stationary turbines, and more, subjected to load spectra with maximum loads of high number of occurrences ($N > 10^6$) and therefore being considered as subjected to constant amplitude loading could be avoided, if the safety factors consider the decrease of fatigue strength. The insight gained is also transferable to the fracture mechanics with the meaning that a threshold stress intensity, ΔK_{th}, does not exist below which, in correlation with a so-called fatigue limit [46], a crack does not grow any more.

References

[1] DS 804 Vorschrift für Eisenbahnbrücken und sonstige Ingenieurbauteile [Regulation for railway bridges and other engineered constructions]. Deutsche Bahn, München; 2000.

[2] FKM-Richtlinie Rechnerische Festigkeitsnachweis für Maschinenbauteile [Analytical proof of strength for machine components]. VDMA-Verlag, Frankfurt am Main; 2002.

[3] AD-Merkblatt S2 Berechnung auf Schwingbeanspruchung [Designing against fatigue] Beuth-Verlag, Berlin/Köln; 1990.

[4] Eurocode No. 3: Design of steel constructions, Part 1. Beuth-Verlag, Berlin; 1993.

[2] Designing against maximum service load and assuming a log-normal distribution, the safety factor j can be calculated for a required probability of failure $P_f = 1 - P_s$ [45]: $j = \left(\frac{1}{T}\right) \exp\left(\frac{(2.36\sqrt{|\lg(1-P_s)|}) - 1}{2.56}\right)$

[5] Eurocode No. 9 Design of aluminium structures, Part 2. Beuth-Verlag, Berlin; 1998.
[6] Dauerschwingversuch DIN 50 100 [Fatigue test]. Beuth Verlag GmbH, Berlin; 1978.
[7] Fischer G, Grubisic V. Dimensioning of wheelset axles – influencing parameters and procedure for the structural durability validation Fraunhofer – Institute for Structural Durability and System Reliability LBF, Darmstadt Report No. FB-226e; 2005.
[8] Sonsino CM, Morgenstern C, Hanselka H. Betriebsfestigkeit von Aluminiumschweißverbindungen unter korrosiven Umgebungsbedingungen im Fahrzeugbau [Structural durability of welded aluminium joints under corrosive environments of automotive engineering]. In: GUS – Tagung Umwelteinflüsse erfassen, simulieren, bewerten (GUS – Conference, determination, simulation, assessment of environmental influences), Pfinztal; 26–28 March 2003, p. 245–56.
[9] Haibach E. Betriebsfestigkeit [Structural durability]. 2nd ed. Düsseldorf: VDI-Verlag; 2002.
[10] Gassner E, Pries H. Zeit- und Dauerfestigkeitsschaubilder für stabartige Bauteile aus Cr-Mo-Stahl, Duraluminium, Hydronaluminium und Elektron [Finite fatigue and endurance limit diagrammes for bar-like components of cr-mo-steel and aluminium alloys]. Luftwissen 1941;8(3):1–4.
[11] Wells JM, Buck O, Roth LD, Tier JK. Ultrasonic fatigue. In: Proceedings of first international conference on fatigue and corrosion. Fatigue up to ultrasonic frequencies. Philadelphia (USA): The Metal Society of AIME; 1982.
[12] Bathias C, Paris PC. Gigacycle fatigue in mechanical practice. New York: Marcel Dekker Publishing; 2006, ISBN 0-8247-2313-9.
[13] Marines I, Dominguez G, Baudry G, Vittori J-F, Rathery S, Doucet J-P, et al. Ultrasonic fatigue tests on bearing steel AISI-SAE 52100 at frequency of 20 and 30 kHz Int. J Fatigue 2003;25:1037–46.
[14] Marines I, Bin X, Bathias C. An understanding of very high cycle fatigue of metals. Int J Fatigue 2003;25:1101–7.
[15] Marines I, Baudry G, Vittori J-F, Rathery S, Doucet J-P, Cantini S et al. Fatigue à tres Grande Nombre de Cycles d'une Gamme Etendue de Materiaux Issus de Differentes Filieres 22e Journee de Printemps, Senlis /France, 21./22; Mai 2003, p. 22.1–8.
[16] Spoljaric D, Danninger H, Weiss B, Chen DL, Ratzi R. Influence of the testing frequency on the fatigue properties of PM-Steels. In: Proceedings of the international conference on deformation and fracture in structural PM materials, Kosice/Slovakia, vol. 1; 1996, p. 147–58.
[17] Stanzl-Tschegg SE. Ultrasonic fatigue. In: Proceedings of the international conference on fatigue 96, vol. III, Berlin; 1996, p. 1887–98.
[18] Stanzl-Tschegg SE, Mayer HR, Tschegg EK, Beste A. In service loading of Al–Si11 aluminium cast alloy in the very high cycle regime. Int J Fatigue 1993;15(4):311–6.
[19] Stanzl-Tschegg SE, Mayer H. Fatigue and fatigue crack growth of aluminium alloys at very high number of cycles. Int J Fatigue 2001;23:231–7.
[20] Mayer H, Papakyriacou M, Pippan R, Stanzl-Tschegg SE. Influence of loading frequency on the high cycle fatigue properties of AlZnMgCu1.5 aluminium alloy. Mater Sci Eng 2001;A314:48–54.
[21] Murakami Y, Namoto T, Ueda T. Factors influencing the mechanism of superlong fatigue failure in steels. Fatigue Fract Eng Mater Struct 1999;22:581–90.
[22] Berger C, Pyttel B, Trossmann T. High cycle fatigue tests with smooth and notched specimens and screws made of light metal alloys. In: Proceedings of the third international conference on very high cycle fatigue. Kusatsu/Japan; Sept. 2004. p. 561–8.
[23] Berger C, Kaiser B. Results of long-term fatigue tests on helical compression springs. In: Proceedings of the third international conference on very high cycle fatigue. Kusatsu/Japan; Sept. 2004. p. 342–9.
[24] Sonsino CM, Kulka C, Huth H. Breitere Verwendung hochwertiger Stahlqualitäten für schwingbeanspruchte Bauteile durch Bereitstellen verlässlicher Kennwerte [Broader use of high quality steels for fatigue loaded structures by means of supplying reliable material data]. Kommission der Europäischen Gemeinschaften, Luxemburg EUR-Report No. 11414 DE. Verlag Bundesanzeiger, Köln; 1988.
[25] Sonsino CM. Einfluss sintertechnischer Grenzen für die Herstellung von schwingbeanspruchten Bauteilen aus Sinterstahl [Effect of sinter technology limits on the manufacturing of fatigue loaded parts from sintered steel]. Fraunhofer-Institut für Betriebsfestigkeit (LBF), Darmstadt LBF-Report No. FB-184; 1989.
[26] Sonsino, CM, Dieterich K. Einfluss der Porosität auf das Schwingfestigkeitsverhalten von Aluminium-Gusswerkstoffen [The effect of porosity on the fatigue behaviour of cast aluminium materials]. Fraunhofer-Institut für Betriebsfestigkeit (LBF), Darmstadt LBF-Report No. FB-188; 1990.
[27] Sonsino CM, Dieterich K. Fatigue design with cast magnesium alloys under constant and variable amplitude loading. Int J Fatigue 2006;28:183–93.
[28] Berg-Pollack A, May U. Einsatz von Leichtmetallen im Kraftfahrzeug [Use of light weight metals in automobiles]. Congress Intelligente Leichtbau Systeme. Hannover; 9/10 2003. p. 1–4.
[29] Adenstedt R. Streuung der Schwingfestigkeit [Scatter of fatigue strength]. Dissertation TU Clausthal; 2002.
[30] Sternkopf J. Dauerfestigkeit von Gusswerkstoffen bei Schwingspielzahlen $>10^7$ [Fatigue limit of cast materials at cycles $>10^7$]. Konstruieren und Gießen 1994;19(3):21–35.
[31] Xu C, Weiss B, Khatibi G, Danninger H. Ultra high cycle fatigue behaviour of high density pm alloy steels. In: Proceedings of the PM 2004 World Congress Vienna; 17–21 October 2004.
[32] Ostermann H. Schwingfestigkeit gekerbter Flachstäbe aus der Aluminiumlegierung AlCuMg2 (3.1354.5) im Bereich zwischen 10^6 und 10^7 Lastspielen [Fatigue strength in the region between 10^6 and 10^7 cycles for notched flat specimens made of aluminium alloy AlCuMg2 (3.1354.5)]. Fraunhofer-Institut für Betriebsfestigkeit (LBF), Darmstadt Technische Mitteilungen [Technical information] TM- No. 38; 1968.
[33] Bacher-Hoechst M, Haydn W, Auweder G. Federn in der Kraftfahrzeugzuliefer- Industrie – Anforderung und Auslegung [Springs in the motor vehicle supply industry – requirements and design] DVM-Report No. 669; 2002. p. 99–107.
[34] Kaufmann H, Wolters DB. Zyklische Beanspruchbarkeit dickwandiger Bauteile aus ferritischem Gusseisen mit Kugelgraphit [Bearable cyclic loading of thick walled parts made of ferritic spheroidal graphite cast iron]. Konstruieren + Gießen 2002;27(1):4–27.
[35] Müller F. Bewertung des Einflusses von Fehlern auf die Schwingfestigkeit von gegossenen und geschweißten Eisenwerkstoffen [Evaluation of the effect of defects on the fatigue strength of cast and welded ferrous materials). Fraunhofer-Institut für Betriebsfestigkeit (LBF), Darmstadt LBF-Report No. FB-205; 1994.
[36] Rethmeier M. MIG-Schweißen von Magnesiumlegierungen [MIG – welding of magnesium alloys]. Dissertation TU Braunschweig; 2000.
[37] Sonsino CM. Über den Einfluss von Eigenspannungen, Nahtgeometrie und mehrachsigen Spannungszuständen auf die Betriebsfestigkeit geschweißter Konstruktionen aus Baustählen [On the effect of residual stress, weld geometry and multiaxial stress states on the structural durability of welded structural steel components]. Materialwissenschaft und Werkstofftechnik 1994;25(3):97–109.
[38] Ritter W, Kenngrößen der Wöhlerlinien für Schweißverbindungen aus Stählen [Characteristics of Wöhler-curves for welded steel joints]. Inst. für Stahlbau und Werkstoffmechanik der TU DarmstadtHeft 53, Dissertation TU Darmstadt; 1994.
[39] Maddox SJ, Razmjoo GR. Fatigue performance of large girth welded steel tubes. In: Proceedings of the offshore mechanics and arctic engineering conference. Material Engineering, OMAE' 98, vol. III. New York: ASME; 1998.
[40] Buitrago J, Weir MS, Kan WC. Fatigue design and performance verification of deepwater risers. In: Proceedings of the offshore mechanics and arctic engineering conference. Materials engineering Paper No. OMAE 2003-37492, OMAE' 03, vol. III. New York: ASME; 2003.

Please cite this article in press as: Sonsino CM, Course of SN-curves especially in the high-cycle fatigue regime ..., Int J Fatigue (2007), doi:10.1016/j.ijfatigue.2006.11.015

[41] Sonsino CM, Maddox SJ, Haagensen P. A short study on the form of the SN-curves for weld details in the high-cycle-fatigue regime IIW-Doc. No. XIII-2045-05; 2005.

[42] Grzesiuk JG. Einfluss der Nahtvorbereitung und Nahtausführung auf die Schwingfestigkeit hochwertiger Aluminiumkonstruktionen [Influence of weld preparation and geometry on the fatigue strength of high-performance aluminium structures]. Dissertation TU Clausthal; 2004.

[43] Sonsino CM, Maddox SJ, Hobbacher A. Fatigue life assessment of welded joints under variable amplitude loading – state of present knowledge and recommendations for fatigue design regulations. In: Proceedings of the 57th annual assembly of IIW international conference. Osaka/Japan; July 15–16, 2004. p. 84–99.

[44] Hobbacher A et al. Recommendations for fatigue design of welded joints and components IIW-Doc. XIII-1539-96/XV-845-96. Abington Cambridge, Woodhead Publishing; 1996 [update 2006].

[45] Filippini M, Dieterich K. An approximate formula for calculating the probability of failure. Fraunhofer-Institut für Betriebsfestigkeit (LBF), Darmstadt Technische Mitteilungen [Technical information] TM – No. 111; 1997.

[46] El Haddad MH, Topper TH, Topper TN. Fatigue life predictions of smooth and notched specimens based on fracture mechanics. J Eng Mater Technol 1981;103(2):91–6.

Please cite this article in press as: Sonsino CM, Course of SN-curves especially in the high-cycle fatigue regime ..., Int J Fatigue (2007), doi:10.1016/j.ijfatigue.2006.11.015